MEaSUREs Northern Hemisphere Polar EASE-Grid 2.0 Daily 6 km Land Freeze/Thaw Status from AMSR-E and AMSR2, Version 1

USER GUIDE

How to Cite These Data

As a condition of using these data, you must include a citation:

Kim, Y., J. S. Kimball, J. Glassy, and K. C. McDonald. 2018, updated 2019. *MEaSUREs Northern Hemisphere Polar EASE-Grid 2.0 Daily 6 km Land Freeze/Thaw Status from AMSR-E and AMSR2, Version 1*. [Indicate subset used]. Boulder, Colorado USA. NASA National Snow and Ice Data Center Distributed Active Archive Center. https://doi.org/10.5067/WM9R9LQ2SA85. [Date Accessed].

FOR QUESTIONS ABOUT THESE DATA, CONTACT NSIDC@NSIDC.ORG

FOR CURRENT INFORMATION, VISIT https://nsidc.org/data/NSIDC-0728

National Snow and Ice Data Center

TABLE OF CONTENTS

1 DATA DESCRIPTION

This Earth System Data Record (ESDR) reports a Northern Hemisphere (NH) Polar EASE-Grid 2.0 record of daily landscape Freeze/Thaw (FT) status derived at 6 km resolution from satellite passive microwave remote sensing using the NASA Advanced Microwave Scanning Radiometer for EOS (AMSR-E) and the JAXA Advanced Microwave Scanning Radiometer 2 (AMSR2) series. The algorithm identifies FT state changes based on the dynamic relationship between brightness temperature (Tb) and changes in the aggregate landscape dielectric constant associated with transitions between predominantly frozen and non-frozen conditions. This FT regional data record augments an existing global 25 km resolution FT-ESDR, the MEaSUREs Global Record of Daily Landscape Freeze/Thaw Status, and provides an approximately four-fold improved spatial resolution over the previous product. This improvement is enabled by processing of orbital swath Tb retrievals closer to the native AMSR-E and AMSR2 36.5 GHz sensor footprint.

1.1 Parameters

The daily AM and PM FT statuses report frozen (0) or thawed (1) conditions in a cell for the corresponding morning or afternoon overpass. In addition to the AM and PM statuses as single values, the FT-ESDR provides a combined (CO) daily classification of the predominantly frozen or non-frozen conditions of the landscape for each grid cell. Four discrete FT metrics are distinguished from the AM and PM Tb retrievals using the following scheme: AM and PM frozen (0); AM and PM thawed (1); AM frozen, PM thawed (2); AM thawed, PM frozen (3). Note that values 2 and 3 occur only in the combined FT status files. The FT-ESDR domain and the associated cold-constraint areas were defined using ERA-Interim daily minimum surface air temperatures (SAT) and a simple cold temperature constraint index (CCI) as described in Kim et al. (2017). Refer to Table 3 for the individual status classifications.

Table 1. FT-ESDR 8-bit Integer Data Identifiers.

Classification	Data Identifiers
Frozen (AM/PM frozen)	0
Thawed (AM/PM thawed)	1
Transitional (AM frozen and PM thawed)	2
Inverse Transitional (AM thawed and PM frozen)	3
No FT status available	252[1]
Non-cold constraint area	253[2]
100% open water	254

[1]Value 252 is used to denote areas with no FT data, for example due to unavailable FT reference states or thresholds.

[2]Value 253 denotes land areas outside of the FT classification domain where ecosystem processes are not significantly affected by cold season constraints, i.e., where the estimated average number of frozen days is less than a minimum threshold of 5 days per year.

1.1.1 Sample Data Record

Refer to Figure 1 for a sample data record of the selected daily combined (CO) FT-ESDR classification results for 2016, where (a) DOY = 100, (b) DOY = 200, (c) DOY = 300, and (d) DOY = 360. White and gray colors denote respective open water bodies and land areas outside of the FT-ESDR domain. The four colors denote AM and PM frozen (FR, blue), AM and PM thawed (NF, red), AM frozen and PM thawed (TR, yellow) and AM thawed and PM frozen (INV-TR, green) status.

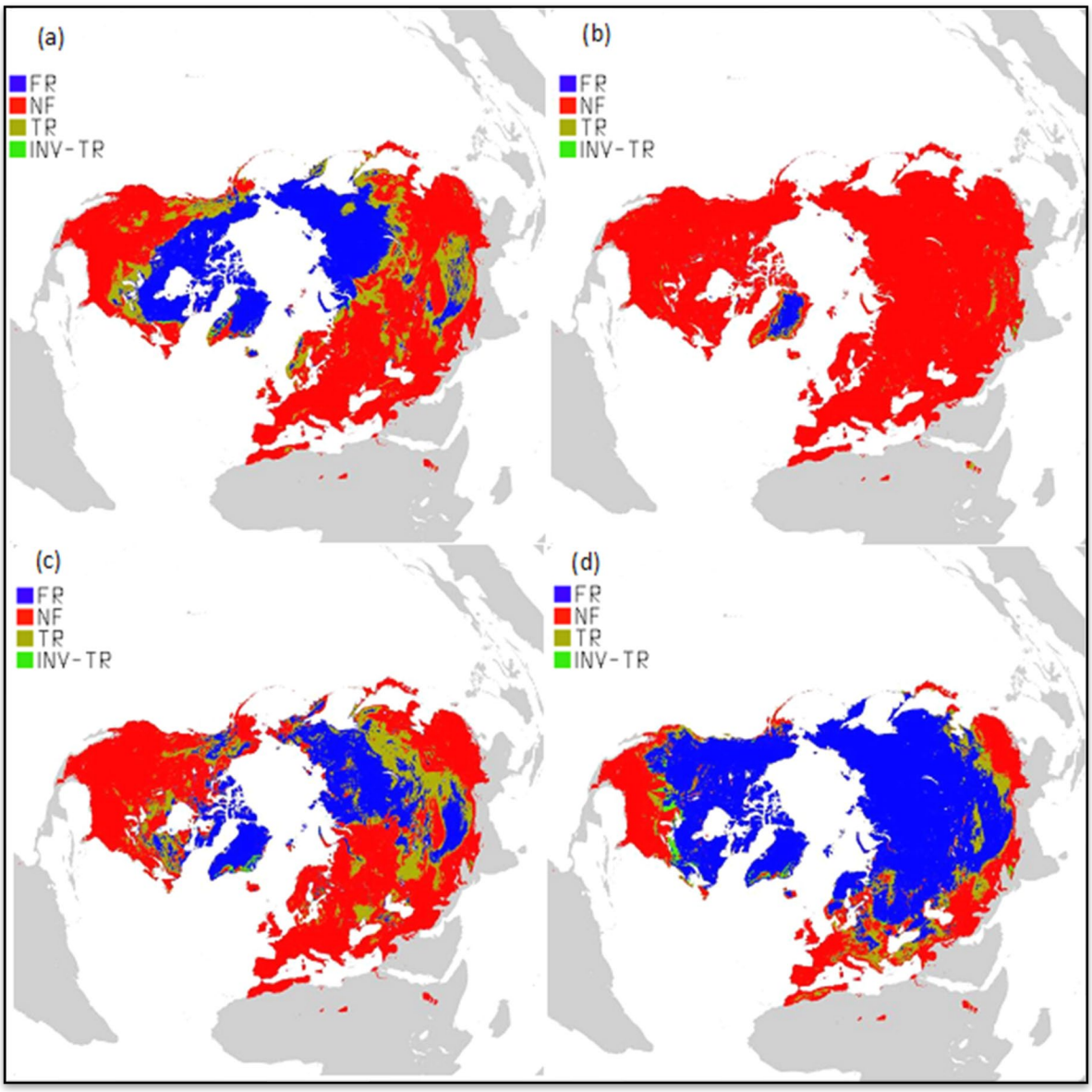

Figure 1. Selected Daily Combined (CO) FT-ESDR Classification Results for 2016.

1.2 File Information

1.2.1 Format

Data are stored in the following formats:

- Binary (.bin)
- GeoTIFF (.tif)

The data consists of 3,000 by 3,000 grid of values, for a total of 9,000,000 pixels, where each value (i.e., each 6-km pixel) is stored

1.2.2 Directory Structure

Data are available from NASA's Earthdata Search or via direct download. When using the direct download option, the top-level directory contains the following subfolders:

/DAILY_BINARY/

- /2002/
- …
- /2017/

/DAILY_GEOTIFF/

- /2002/
- …
- /2017/

/ANNUAL_BINARY_QA/

- /2002/
- …
- /2017/

The /DAILY_BINARY/ and /DAILY_GEOTIFF/ subfolders contain the daily records of landscape Freeze/Thaw status. The /ANNUAL_BINARY_QA/ subfolder contains annual quality assurance (QA) maps describing the relative quality of the PER Freeze/Thaw classification.

1.2.3 Naming Convention

Files in /DAILY_BINARY/ and /DAILY_GEOTIFF/ follow the same naming convention, whereas files in /ANNUAL_BINARY_QA/ follow a slightly different convention. Variables the file names are defined in Table 2 below.

Example File Names

- `AMSR_36V_PM_FT_2002_day357_NH_06km_v01.bin`
- `AMSR_36V_AM_FT_2013_day359_NH_06km_v01.tif`
- `AMSR_36V_PM_QA_2017_NH_06km_v01.bin`

The file `AMSR_36V_PM_FT_2002_day357_NH_06km.bin` represents the AMSR sensor at 36.5 GHz, vertically polarized Tb-based FT classification, for composite daily conditions on day 357 of 2002 over the Northern Hemisphere domain at 6 km spatial resolution.

Naming Conventions

`[InstrumentLabel]_[Channel][Polarization]_[OverpassCode]_FT_[Year]_day[DOY]_NH_06km_[Version].[FileExt]`

`[InstrumentLabel]_[Channel][Polarization]_[OverpassCode]_QA_[Year]_NH_06km_[Version].[FileExt]`

Table 2. File Name Variables and Definitions.

Variable	Definition
`InstrumentLabel`	Sensor: AMSR (for both AMSR-E and AMSR2)
`Channel`	Frequency (GHz): 36
`Polarization`	V (vertical)
`OverpassCode`	Morning overpass (AM), evening overpass (PM), or combined daily AM and PM overpass (CO)
`Year`	4-digit observation year
`DOY`	Day of year
`Version`	v01 (example)
`FileExt`	.bin (binary) .tif (GeoTIFF)

1.2.4 File Size

The total file volume of `.bin` files is approximately 3.9 GB.

The total file volume of `.tif` files is approximately 4 GB.

The total data set volume is approximately 8.2 GB.

1.3 Spatial Information

1.3.1 Coverage

The geographical range encompasses the Northern Hemisphere.

Northernmost Latitude: 90°N
Southernmost Latitude: 0°N
Easternmost Longitude: -180°W
Westernmost Longitude: 180°W

The FT-ESDR domain encompasses all Northern Hemisphere land areas affected by seasonal frozen temperatures, including urban, barren land, snow-ice, and open water body dominant grid cells.

1.3.2 Resolution

Data are gridded at 6 km.

1.3.3 Projection and Grid Description

The data are projected using a polar aspect Lambert azimuthal equal-area projection with the WGS 84 datum (EASE-Grid 2.0 North; Brodzik et al. 2014). The EPSG code for this projection is 6931. Refer to Table 3 for the defining pixel coordinates of the 6-km grid used with this projection.

Table 3. Grid Coordinates

Location in grid	Pixel
Upper left corner	-9,000,000; 9,000,000
Lower left corner	-9,000,000; -9,000,000
Upper right corner	9,000,000; 9,000,000
Lower right corner	9,000,000; -9,000,000
Center	0; 0

1.4 Temporal Information

1.4.1 Coverage

02 June 2002 to 31 December 2017

1.4.2 Resolution

Daily

2 DATA ACQUISITION AND PROCESSING

2.1 Theory of Measurements

The FT state parameter quantifies the predominant frozen or non-frozen state of the landscape and is closely linked to changes in the surface energy budget and evapotranspiration (Zhang et al.

2011), vegetation growth and phenology (Kim et al. 2014a), snowmelt dynamics (Kim et al. 2015), permafrost extent and stability (Park et al. 2016), terrestrial carbon budgets and land-atmosphere trace gas exchange (Kim et al. 2014b). Satellite-borne passive microwave sensors are particularly well-suited to monitoring global FT status of the landscape because they are strongly sensitive to changes in dielectric properties at the surface that correspond to frozen and thawed states, are relatively insensitive to atmospheric contamination, and do not require solar illumination. The following sections outline the approach used to infer FT state changes from remotely sensed Tb. For a complete description, see Kim et al. (2011).

2.2 Acquisition

The AMSR-E 36.5 GHz orbital swath Tb data have a native footprint resolution of 14 km x 8 km (Kawanishi et al., 2003), while the similar frequency Tb orbital swath (L1R) data from AMSR2 have a native 12 km x 7 km footprint resolution (Imaoka et al. 2010; Imaoka et al. 2012). The AMSR-E and AMSR2 swath Tb data were re-projected to a 6 km polar EASE-Grid 2.0 projection format using an Inverse Distance Squared spatial interpolation approach following previously established methods (Du et al. 2017).

The data were primarily derived using similar calibrated overlapping daily morning (AM) and afternoon (PM) overpass radiometric Tb measurements at 36.5 GHz (V-pol) frequency from the AMSR-E and AMSR2 series. The resulting FT-ESDR represents a consistent, daily FT polar record that extends over a 16-year (2002 to 2017) observation period, ensuring cross-sensor consistency through double-differencing calibration of AMSR2 to AMSR-E Tb records (Du et al. 2014). Double-differencing calibration was conducted using similar frequency collocated overlapping Tb records from the FY-3B Microwave Radiation Imager (MWRI), which was applied to fill the temporal Tb gaps for 2011-2012 period (Du et al. 2014).

2.3 Derivation Techniques and Algorithms

The FT classification algorithm uses a temporal change detection of radiometric Tb time-series that identifies FT transition sequences by exploiting the dynamic temporal Tb response to differences in the aggregate landscape dielectric constant that occur as the landscape transitions between predominantly frozen and non-frozen conditions (McDonald and Kimball 2005; Kim et al. 2011; Kim et al. 2012). Satellite ascending and descending orbital Tb time series are processed separately to produce information on AM, PM and composite daily FT conditions (CO). Additional variables distinguished by the FT-ESDR include transitional (AM frozen and PM thawed) or inverse transitional (AM thawed and PM frozen) conditions. Detailed descriptions of the FT-ESDR methods, algorithm performance, and product accuracy are provided by Kim et al. (2017).

2.4 Instrumentation

2.4.1 Description

The Advanced Microwave Scanning Radiometer - Earth Observing System (AMSR-E) is a twelve-channel, six-frequency, passive-microwave radiometer system aboard the NASA Earth Observing System Aqua Satellite. The instrument measures horizontally and vertically polarized Tb at 6.9 GHz, 10.7 GHz, 18.7 GHz, 23.8 GHz, 36.5 GHz, and 89.0 GHz. Spatial resolution of the individual measurements varies from 5.4 km at 89 GHz to 56 km at 6.9 GHz. AMSR-E was developed and provided by the Japan Aerospace Exploration Agency (JAXA, Contractor: Mitsubishi Electric Corporation) with close cooperation of U.S. and Japanese scientists. The AMSR-E instrument aboard Aqua was modified from the design used for AMSR, which flew on the Japanese ADEOS-2 satellite. See NSIDC's AMSR-E Instrument Description technical document for more information.

The Advanced Microwave Scanning Radiometer 2 (AMSR2) was launched aboard the Global Change Observation Mission (GCOM-W1) satellite on 17 May 2012. The AMSR2 antenna rotates once every 1.5 seconds and obtains data over a 1,450 km swath. This configuration acquires a set of daytime and nighttime data every two days that covers more than 99 percent of the Earth. Except for a 7.3 GHz channel designed to mitigate radio frequency interference, the AMSR2 channel set is identical to AMSR-E.

The Microwave Radiation Imager (MWRI) is one of the eleven instruments aboard the Feng Yun 3B (FY-3B) satellite, which was launched on 05 November 2010 (Yang et al. 2011). FY-3B is the second satellite of the FY-3 series, China's second-generation polar-orbiting meteorological satellites. MWRI observations are used to bridge the temporal gap between AMSR-E and AMSR2 measurements and are based on similarly calibrated 36.5 GHz Tb retrievals.

3 SOFTWARE AND TOOLS

GeoTIFF files may be viewed with the following tools: ESRI ArcGIS, QGIS, or Other Geographical Information System (GIS) software.

VERSION HISTORY

Version 1.1 was released November 2020. Refer to Table 3 for the data set version history:

Table 4. Version History Summary

Version	Release Date	Description of Changes
V1	December 2017	Initial release
V1.1	November 2020	In version 1.1, daily binary files from 01 January 2017 to 31 December 2017 have been replaced with updated versions due to the discovery of bad PER FT values in the original files. The bad data appears to be isolated to the months of March-December. All data for 2017 was replaced as a precaution.

4 RELATED DATA SETS

- MEaSUREs Global Record of Daily Landscape Freeze/Thaw Status

5 RELATED WEBSITES

- Freeze/Thaw Earth System Data Record

6 CONTACTS AND ACKNOWLEDGMENTS

Youngwook Kim, John S. Kimball, Jinyang Du, and Joseph Glassy
Numerical Terradynamic Simulation Group (NTSG)
The University of Montana
Missoula, MT 59812, USA
E-mail: youngwook.kim@umontana.edu; john.kimball@umontana.edu; jinyang.du@umontana.edu; um.glassy@gmail.com

Project URL: http://freezethaw.ntsg.umt.edu/

Technical Contact
NSIDC User Services
National Snow and Ice Data Center

CIRES, 449 UCB
University of Colorado
Boulder, CO 80309-0449, USA
Phone: +1 (303) 492 6199
Fax: +1 (303) 492 2468
E-mail: nsidc@nsidc.org

Acknowledgments

These data were generated through a grant from the NASA MEaSUREs (Making Earth System Data Records for Use in Research Environments) program (NNX14AB20A). This work was conducted at the University of Montana under contract to NASA.

7 REFERENCES

Brodzik, M. J., B. Billingsley, T. Haran, B. Raup, and M. H. Savoie. 2014. Correction: Brodzik, M. J., et al. EASE-Grid 2.0: Incremental but Significant Improvements for Earth-Gridded Data Sets. ISPRS *International Journal of Geo-Information*, 3 (3), 1154-1156. https://doi.org/10.3390/ijgi3031154.

Du, J., J. S. Kimball, C. Duguay, Y. Kim, and J. D. Watts. 2017. Satellite microwave assessment of Northern Hemisphere lake ice phenology from 2002 to 2015. *The Cryosphere*, 11, 47-63. https://doi.org/10.5194/tc-11-47-2017.

Du, J., J. S. Kimball, J. Shi, L. A. Jones, S. Wu, R. Sun, and H. Yang. (2014). Inter-calibration of satellite passive microwave land observations from AMSR-E and AMSR2 using overlapping FY3B-MWRI sensor measurements. *Remote Sensing*, 6, 8594-8616. https://doi.org/10.3390/rs6098594.

Imaoka, K.; Takashi, M.; Misako, K.; Marehito, K.; Norimasa, I.; Keizo, N. 2012. Status of AMSR2 instrument on GCOM-W1. *Earth Observing Missions and Sensors: Development, Implementation, and Characterization*, 852815. http://dx.doi.org/10.1117/12.977774.

Imaoka, K., M. Kachi, M. Kasahara, N. Ito, K. Nakagawa, and T. Oki. 2010. Instrument performance and calibration of AMSR-E and AMSR2. *ISPRS Archives*, 38, 13-18.

Kawanishi, T. J., T. Sezai, Y. Ito, K. Imaoka, T. Takashima, Y. Ishido, A. Shibata, M. Miura, H. Inahata, and R. W. Spencer. 2003. The advanced scanning microwave radiometer for the EarthObserving System (AMSR-E): NASDA's contribution to the EOS for global energy and water cycle studies. *IEEE Transactions on Geoscience and Remote Sensing*, 41, 184-194. https://doi.org/10.1109/TGRS.2002.808331.

Kim, Y., J. S. Kimball, J. Glassy, and J. Du. 2017. An Extended Global Earth System Data Record on Daily Landscape Freeze-Thaw Determined from Satellite Passive Microwave Remote Sensing, Earth System Science Data, 9, 133-147. https://doi.org/10.5194/essd-9-133-2017.

Kim, Y., J. S. Kimball, D. A. Robinson, and C. Derksen. 2015. New satellite climate data records indicate strong coupling between recent frozen season changes and snow cover over high northern latitudes. *Environmental Research Letters*, 10, 084004. https://doi.org/10.1088/1748-9326/10/8/084004.

Kim, Y., J. S. Kimball, K. Didan, and G. M. Henebry. 2014a. Responses of vegetation growth and productivity to spring climate indicators in the conterminous Unites States derived from satellite remote sensing data fusion. *Agricultural and Forest Meteorology*, 194, 132-143. https://doi.org/10.1016/j.agrformet.2014.04.001.

Kim, Y., J. S. Kimball, K. Zhang, K. Didan, I. Velicogna, and K. C. McDonald. 2014b. Attribution of divergent northern vegetation growth responses to lengthening non-frozen seasons using satellite optical-NIR and microwave remote sensing, *International Journal of Remote Sensing*, 35, 3700-3721. https://doi.org/10.1080/01431161.2014.915595.

Kim, Y., J. S. Kimball, K. Zhang, and K. C. McDonald. 2012. Satellite detection of increasing northern hemisphere non-frozen seasons from 1979 to 2008: Implications for regional vegetation growth. *Remote Sensing of Environment*, 121, 472-487. https://doi.org/10.1016/j.rse.2012.02.014.

Kim, Y., J. S. Kimball, K. C. McDonald, and J. Glassy. 2011. Developing a Global Data Record of Daily Landscape Freeze/Thaw Status using Satellite Microwave Remote Sensing. *IEEE Transactions on Geoscience and Remote Sensing*, 49, 949-960. https://doi.org/10.1109/TGRS.2010.2070515.

McDonald, K. C, and J. S. Kimball. 2005. Hydrological application of remote sensing: Freeze-thaw states using both active and passive microwave sensors. *Encyclopedia of Hydrological Sciences. Part 5. Remote Sensing*. M.G. Anderson and J.J. McDonnell (Eds.), John Wiley & Sons Ltd. https://doi.org/10.1002/0470848944.hsa059a.

Park, H., Y. Kim, and J. S. Kimball. 2016. Widespread permafrost vulnerability and soil active layer increases over the high northern latitudes inferred from satellite remote sensing and process model assessments. *Remote Sensing of Environment*, 175, 349-358. https://doi.org/10.1016/j.rse.2015.12.046.

Yang, H., F. Weng, L. Lv, N. Lu, G. Liu, M. Bai, Q. Qian, J. He, H. Xu. 2011. The FengYun-3 microwave radiation imager on-orbit verification. *IEEE Transactions on Geoscience and Remote Sensing*, 49, 4552-4560. https://doi.org/10.1109/TGRS.2011.2148200.

Zhang, K., J. S. Kimball, Y. Kim, and K. C. McDonald. 2011. Changing freeze-thaw seasons in northern high latitudes and associated influences on evapotranspiration. *Hydrological Processes*, 25, 4142-4151. https://doi.org/10.1002/hyp.8350.

8 DOCUMENT INFORMATION

8.1 Publication Date

11 December 2017

8.2 Date Last Updated

October 2021